Civil Engineering Research Journal
ISSN: 2575-8950

Juniper Publishers
key to the Researchers

Review Article
Volume 3 Issue 3 - February 2018
DOI: 10.19080/CERJ.2018.03.5555611

Civil Eng Res J

Visual Interpretation of DEM Fill Mechanisms for a Rope Shovel Dipper in Dry Broken Rock

Curley M*, Joseph TG and Rasimarzabadi R

Department of Civil & Environmental Engineering, University of Alberta, Canada

Submission: November 11, 2017; **Published:** February 13, 2018

***Corresponding author:** Curley M, Department of Civil & Environmental Engineering School of Mining & Petroleum Engineering Markin/CNRL Natural Resources Engineering Facility 9105 116th St Edmonton, Alberta, T6G 2W2, Canada, Email: mcurley@ualberta.ca

Abstract

A discrete element model (DEM) particle flow code (PFC) based 2D numerical simulation was used to model the behaviour of crushed cohesion-less rock fragments passing into a rope shovel dipper (bucket); mimicking previous field verified physical 1/32nd scale tests. While the previous physical tests showed the development of a previously unknown void space within the dipper that perpetuated low dipper fill factors; the model reported in this paper was developed to show the impact of particle size characteristics on the ability of a given shovel dipper geometry to fill, within a set arc dig trajectory.

In comparison to the previous scale physical tests, a good correlation to the DEM indicated that the numerical method was able to mimic the dipper fill process; specifically particle flow mode sand development of flow layers and particle obstructions, akin to sanding in a low velocity hydro-transport pipeline.

Keywords: Rope shovel; Particle flow; Simulation; Discrete element method; PFC; Dipper

Introduction

A particle flow code (PFC) based discrete element model (DEM) presents a viable tool to numerically model ground engaging tool interactions; which may be used to mimic and predict complex surface versus media concerns that are manifest as low productivity KPIs [1]. Such DEM methods have been widely used to predict the flow behaviour of rock materials for several decades, providing tangible solutions for industrial and mining problems [2].

Coetzee et al. [1-5] modeled the flow of broken rock particles into a dragline dipper using DEM, proposing a means of estimating the input parameters required for the modeling of cohesion-less material, where the size and density of particles were assessed through direct measurement. Coetzee et al. [1-5] showed that particles for a range of frictional and size characteristics could be represented by clumps of varying size PFC spherical particles interacting with one another. This early work was verified through mimicking of a confined compression test [1]. However, Coetzee et al. [1,3-5] concluded that although a general modeling trend was indicated, the DEM was unable to predict the dragline bucket-ground interaction with the anticipated accuracy[1,3-5].

Cleary [6,7] in preceding the work of Coetzee et al. [1,3- 5], modelled the fill process for a dragline dipper using DEM to compare the loading for different dragline bucket designs, and to evaluate the loading impact on the dragline bucket hoist and drag rope system. Cleary specifically of interest for this paper, studied the effect of particle shape on fill times and bucket fill volumes achieved, noting the two rock shape parameters of aspect ratio and sharpness appeared to greatly influence the behaviour of a particle's ability to fill a dragline bucket [2,8], modelled via PFC encoded spheres and spherical based super-quadric hybrid shapes in DEM-3D [8,9]. Cleary's results indicated that non-spherical particles showed more resistance to flow, more representative of the friction resistance of rock particles to flow resulting in lower fill factor payloads, but with an increased fill time [9]. In parallel work, Owen et al. [10] simulated a dragline bucket fill, where particles were modeled via DEM-3D and the bucket load response was modeled via finite element modelling [10], such that drag forces and trajectory distances were shown comparable with a scale physical test.

Following the work of Coetzee et al. [1,3-5], Cleary [2, 6- 9] and Owen [10], this paper will show a parallel DEM application to investigating the flow of broken rock particles into a rope shovel dipper, where there is strong correlation to 1/32nd scale physical tests using a transparent dipper and test bin, permitting the visual inspection of material behaviour as previously reported by Rasimarzabadi & Joseph [11].

DEM as applied to a shovel dipper passing through a digging medium, then employs two principal elements to define rock

particles and the shovel dipper rigid body; as spheres and walls respectively [12,13]. In 2D simulations, a sphere is a stiff circle with unit thickness; while in 3D simulations, a true spherical shape is defined [14]. To model non-circular (non-spherical) particles that may then be attributed higher surface frictional properties, as might be expected for highly angular broken rock fragments in a blasted rock file under shovel dipper excavation; clumps of multi-sized spheres were used, where a clump was a combination of two or more spheres that remained rigid under all modeled conditions [14].

To provide a comparator and by extension a scaled validation of the DEM numerical results, a set of scaled physical tests were performed, after Rasimarzabadi & Joseph [11], using a transparent scaled rope shovel dipper and test bin arrangement (Figure 1). The scale testing was based on well accepted physical testing scaling laws as reported by Ghosh & Chakraborty [15]. The 1/32nd volumetric cube root scaled dipper model referenced a 44m3 ultra-class category field scale dipper found on Komatsu P&H4100 and Caterpillar 7495 model electric rope shovels in common large scale surface mine hard rock operations. The scaled dig medium was constructed from crushed dolomitic limestone rock mimicking the field particle size distribution relative to the shovel dipper geometry. As such, the field mean rock particle size of 0.380.32m relative to a 44m3 capacity dipper with a 3.58m wide lip set the 1/32nd scale 1,340 cm3 capacity dipper with a 11 cm wide lip and 1.21 cm mean size broken rock. The dolomitic limestone was chosen as it fractured under crushing producing similar angularity and surface roughness commensurate with a field hard rock blast excavation face.

The scale dipper hoist system was effected in a similar arc trajectory to that experienced by the field rope shovel system, relative to a 1/32nd scaled dig trajectory for the same dig cycle time experienced in the field, such that a dig velocity range from 0.450.5 to 0.951m/s was then set at 1.41.6 to 3.03.1cm/s. The transparent wear bin dig face height was also scaled from 12m in field to 37.5cm in height at a similar angle of repose of 38, (Figure 1). With all geometries scale matched from field to test scenario, the flow mechanisms generated through the dipper to dig face interactions were then commensurate with the field conditions, permitting high speed camera visual observation of the particle flow characteristics into and around the scale dipper as it passed through the dig face material. Specific operation details for the testset-upmay be found in Rasimarzabadi [16] and Rasimarzabadi & Joseph [11].

Figure 1: Scale physical test transparent test bin and dipper system.

Defining Model Particle Material Properties

Although DEM simulation relies on micro- rather than macro-properties of materials, where micro-properties of materials with simple packing arrangements such as spherical contacts may be predicted from material macro-properties; it is more difficult to determine broken rock particle material properties, where arbitrary particle orientations are present. In this instance, to assign appropriate micro-property values for broken rick rock particles, calibration methods are required; where density, particle shape, particle size distribution, shear stiffness and friction define those micro-properties [1,13,17]. For example, apparent (broken rock) density may be determined and used as an appropriate particle density for PFC modeling purposes [18].

In DEM models, particles are represented by discs (2D) or spheres (3D). Such particles do not represent broken rocks well. However, DEM is capable of modeling particles with non-circular, non-spherical shapes by creating clumps of discs or spheres of different size and configuration [14]. To determine the representative shape of particles commensurate with that used kin the scale physical tests, a random sample of 250 particles was taken from the dig face material. These particles were classified into three groups based on their overall shape. For simplicity, where complexity of modeled particle is directly proportional to computing power needed to run a given model, the classification was restricted to three clumped particles designed for PFC use. Figure 2 shows the three shapes designed to mimic the broken rock particles relative to frequency of occurrence in the dig face.

How to cite this article: Joseph TG, Rasimarzabadi R, Curley M. Visual Interpretation of DEM Fill Mechanisms for a Rope Shovel Dipper in Dry Broken Rock. Civil Eng Res J. 2018; 3(3): 555611. DOI: 10.19080/CERJ.2018.03.5555611

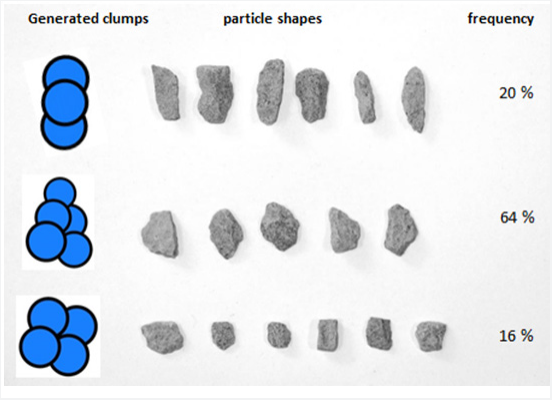

Figure 2: Particle shapes designed for broken rock PFC model.

To determine the 1/32nd test size distribution for the crushed dolomitic limestone, the digital image processing system, WipFrag, was used, generating the distribution in Figure 3; compared with the field dig face blast size distribution being mimicked and the PFC model size distribution. A user defined FISH function was written to model the scaled up results from Wipfrag, producing a comparable match to the scale and actual rock particle distribution.

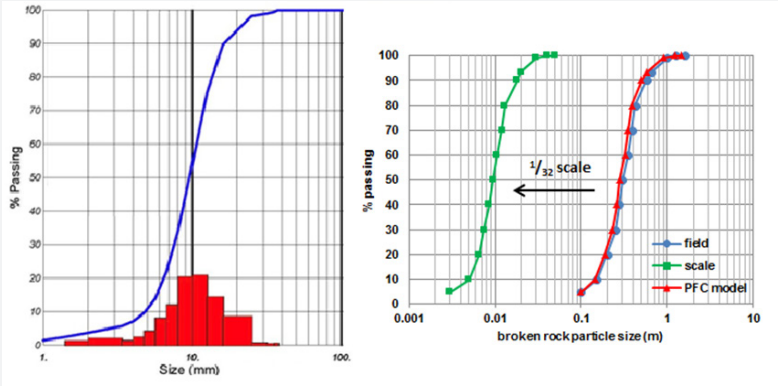

Figure 3: Size distribution of crushed dolomitic limestone relative to field case and PFC model.

In order to estimate particle to particle model stiffness commensurate with the actual material frictional and geometric contacts, a simple packing simulation was conducted, where particles fall into a container under gravity and settle to equilibrium. As such, it was assumed that normal and shear stiffness were equal. The stiffness model comprised eight containers filled with particles of similar characteristics but different stiffness. The model was influenced by the shape and size distribution of the rock particle fragments used in the physical test.

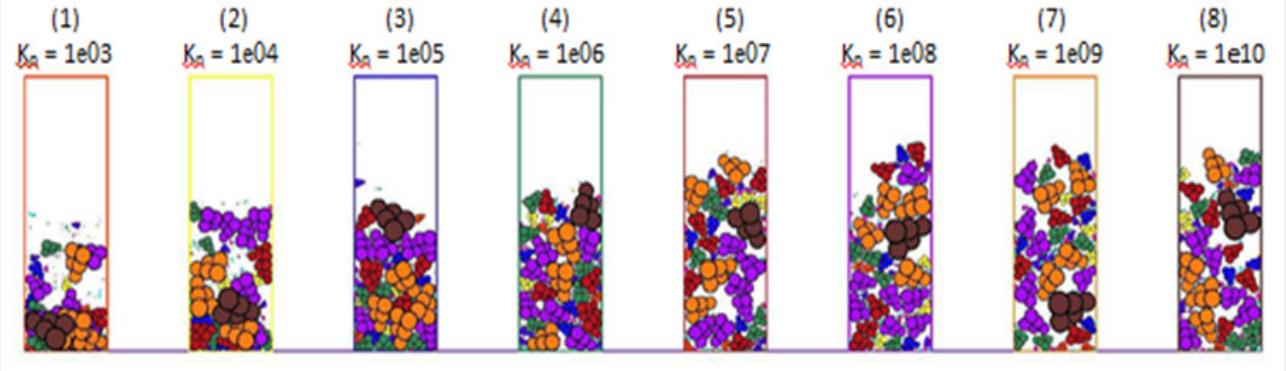

Figure 4: Particle packing of different stiffness.

How to cite this article: Joseph TG, Rasimarzabadi R, Curley M. Visual Interpretation of DEM Fill Mechanisms for a Rope Shovel Dipper in Dry Broken Rock. Civil Eng Res J. 2018; 3(3): 555611. DOI: 10.19080/CERJ.2018.03.5555611

In Figure 4, container 1 presented the lowest particle stiffness, with large void spaces. Increasing the particle stiffness in containers 2 through 8, from left to right, it was observed that the height of particles in the containers proportionally increased, resulting from decreased particle overlap. It was also observed that a proportional change in stiffness (columns 5 through 8), had a minimal impact on the change of particle height in the container. Majidi [17] argued that where stiffness change had a minimal impact, the particles were then compacted with minimal overlap. To reduce the model computational time step, a minimal value of stiffness was selected at kn= ks = 1exp06.

The broken rock particle to particle friction coefficient is a critical parameter in establishing the angle of repose of the dig face in numerical modeling using PFC. Since the angle of repose is a reasonable indicator of an effective friction co-efficient for cohesion less broken rock fragments, the angle of repose was used to indicate the friction co-efficient [19]. The dolomitic limestone particles used in the physical test were poured onto a horizontal surface, (Figure 5). The pile conic angle relative to the horizontal was taken as the angle of repose of broken material. For a number of piles, a mean angle of repose was determined. The pile angle of repose test was simulated in PFC2D for different friction coefficients, revealing outcomes comparable to the physically measured angle of repose and focusing on an appropriate friction coefficient value for simulating the dolomitic limestone broken rock.

Figure 5: Dolomitic limestone particles piled at 38oangle of repose.

Frictional sliding between the components of a system reduces the energy of the system; but frictional sliding alone is insufficient to establish a state of equilibrium in a model [14]. Local damping and viscous damping are two options to reduce kinetic energy in PFC; where local damping generates a damping force on each particle that has a value comparable to an unbalanced force, while viscous damping provides a damping force comparable to the relative velocity difference between two particles in contact [14].When a system needs to rapidly reach an equilibrium state, local damping works best [13]. For systems with dynamic behaviour, or systems where particles are free to move in the domain area, viscous damping is more suitable [14].

However, damping is a property that does not have a specific calibration method [13]. Here a set of test runs were conducted to evaluate different damping coefficients. Analysis of the results implied that both local and viscous damping was potentially needed. Viscous damping was a good option for systems involving free flowing rock particles, as is the case here; once establishment of the dig face file pile was achieved, leveraging local damping to establish a reasonably steep dig slope angle of repose. The local damping coefficient absorbed undesirable energy generated when establishing the dig face pile as material dropped onto a horizontal surface which under un damped conditions would generate a low rock material angle of repose.

Processing Time

In DEM, the total processing time depends on computer processor power. Long simulation periods revealed that it was necessary to employ appropriate strategies to shorten total processing time. In PFC, two parameters that may be manipulated to control simulation time are the time step and cycle time [13].

The process duration, a function of the simulation setup and complexity of parameters, may be shortened by [13] reducing the quantity of objects in the system, including modeling spheres, clumps, and walls and reducing the time taken to generate the rock particles and dig face from spheres and clumps. Here, the number of calculations performed per cycle was reduced by decreasing the number of rock clump particles and number of shovel dipper and dig bin walls in the system. As such, the dipper was modeled as the simplest geometry possible, Figure 6 and generation of highly complex particle clump shapes were avoided.

How to cite this article: Joseph TG, Rasimarzabadi R, Curley M. Visual Interpretation of DEM Fill Mechanisms for a Rope Shovel Dipper in Dry Broken Rock. Civil Eng Res J. 2018; 3(3): 555611. DOI: 10.19080/CERJ.2018.03.5555611

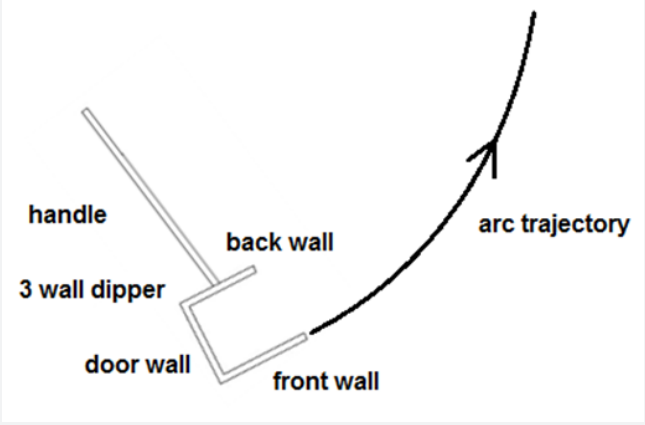

Figure 6: Simplified handle and 3 wall dipper arrangement for PFC model.

Generating a broken rockpile with a broad size distribution of particle sizes and shapes adversely extended the model computational processing time, given the large proportion of generated clumps required in the system, thus limiting the number of runs possible. As such, rather than generate the entire DEM broken rockpile from clumps, the rock particle to dipper contact zone was focused as a capping layer of set thickness over a set linear slope at the angle of repose.

To further reduce the processing time, the time step was increased. In a linear contact model, the time step is dependent on particle stiffness, density, and size [13]. A lower stiffness results in a smaller time step; however, small magnitude stiffness causes unrealistic overlaps between spheres and clumps as evident from (Figure 4), [17]. It should be borne in mind that conversely a higher stiffness may also result in unrealistic behaviour, due to high forces generated between two particles in contact [17].

DEM Simulation Material Flow Into A Rope Shovel Dipper

Once the particles for the surface layer of the rockpile were created, they were permitted to reach an equilibrium state. The dipper was then created into the model using rigid walls, initiated in the model at the toe of the rockpile. The dipper was then moved through the particle layer by assigning a rotational speed to the dipper walls. The motion behaviour of the particles and the loading flow mechanism were recorded, and compared to the experimental test observations reported by Rasimarzabadi & Joseph [11].

The results indicated good correlation to the dipper – material flow filling process seen in the physical tests [11]. It was specifically observed, as a qualitative key indicator of modeling success, that as the dipper engaged the rockpile, a thin layer of material flowed into the dipper (flow zone), with particles rotating and sliding relative to each other. An increase in broken rock pile penetration by the dipper, prior to moving along the trajectory path, resulted in greater material being displaced and flowing into the dipper, proportional to an increased thickness in flow zone.

As more rock particles entered the dipper, those adjacent to the inner dipper walls, interlocked to particles that they came into contact with, generating a bulk larger volume zone moving much slower into the dipper, while the previously identified flow zone was now forced to flow over the slower moving bulk zone. The closet analogy to this would be 'sanding' in a slurry pipeline, where solids of larger mass or density drop out of the main flow regime and create a restricting pile in the base of a pipeline, impeding the ongoing flow of a slurry. The simulation here clearly showed the mode of two motions as the flow and bulk zones.

Observed both in the physical tests [11] and in the model here, the flowing material into the dipper generated a flow restricting pile, inside the leading edge (lip) of the dipper front wall, which progressively increased in size through the dig cycle. Given the progressively increasing restriction as the dig cycle progressed along the dipper trajectory, a void space was generated at the contact between the back and door walls of the dipper. As the restriction increased in size, less material was able to progress in the flow zone to fill the dipper, and hence the void space became inaccessible to fill. In the physical test [11] it was observed that the void space remained set to the point at which the thickness of the flowing material over the bulk zone approached the back wall of the dipper. In rotating the dipper as it proceeded to the end of its trajectory and broke out of the dig face, the material contained in the front of the dipper sloughed into the void space, effectively transferring the void from back-door corner to back-front opening zone.

Although the numerical model was successful in simulating the general flow pattern, it had some restrictions in reproducing the physical test results. Figure 7 compares the results of the DEM model versus the physical test.

How to cite this article: Joseph TG, Rasimarzabadi R, Curley M. Visual Interpretation of DEM Fill Mechanisms for a Rope Shovel Dipper in Dry Broken Rock. Civil Eng Res J. 2018; 3(3): 555611. DOI: 10.19080/CERJ.2018.03.5555611

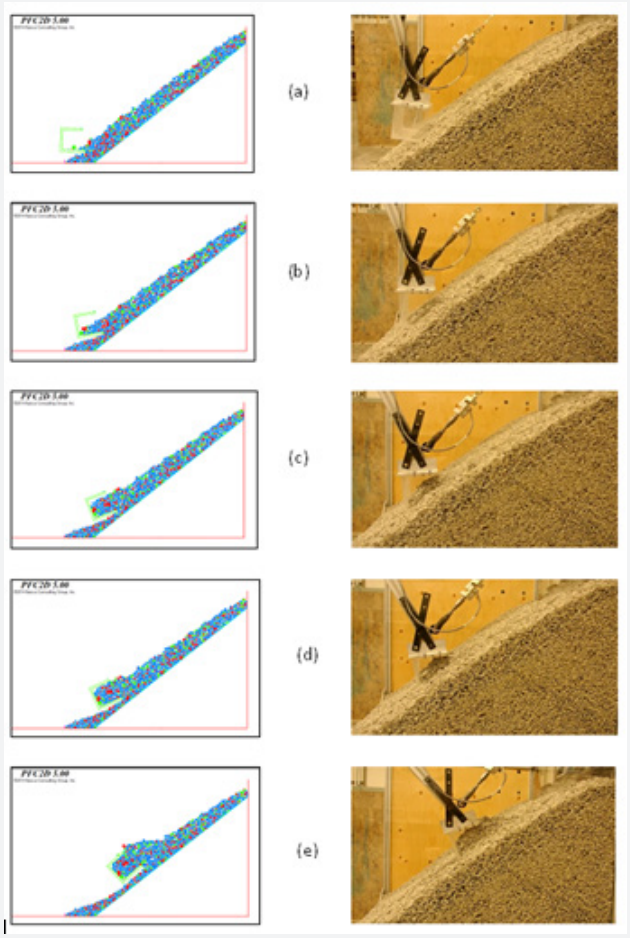

Figure 7: Dipper filling comparison: DEM vs physical test.

Figure 7a shows the dig cycle initiation, where the dipper first engages the broken rock dig face pile. The DEM seems to have reasonably simulated this segment. Figure 7b then illustrates the point at which the flow zone material contacts the rear-door of the dipper. Although the height of material at the dipper's ingress appears the same in the physical test and numerical model, the particle slope forming inside the dipper appears more shallow in the simulation.

In progressing through the dig cycle, a wedge of particles inside the ingress at the front wall of the dipper is formed, the thickness of which progressively increases, but again with an apparent pile slope noticeably reclined in the numerical model. This results in a much smaller void space developing at the rear of the simulated dipper, Figure 7-c and Figure 7d. As the thickness of the material obstruction at the dipper ingress reaches the dipper back wall, the size of the void space in the DEM model becomes insignificant Figure 7e.

The DEM model results did indicate that although the simulated material showed the same flow pattern as evidenced by the physical test results, it did not adequately mimic the void space generation that consistently impacts fill factor for such shovel dippers in industry. It is evident that the simulated particles moved past one another with a much lower fictional resistance than anticipated, and as such did not behave as angular, rough particles. This resulted in a lower angle of repose pile of material developing inside the front wall of the dipper, and a smoother flow of particles than the physical test case, more easily able to fill the void space at the rear of the dipper.

On reflection, the model was hampered by poor assumptions of particle behaviour

a. Roughness of particles: In an attempt to generate rough particles via more complex clump geometries, the computing power limited complexity. Simple clumps were chosen, but were not complex enough to generate the roughness and friction response expected. As surface roughness increases, the value of the inter-particle friction coefficient increased which lead to reducing rolling ability and increased interlocking; where as smooth particles were able to move past one another via sliding and rotation with only limited resistance.

b. Friction coefficient: The inter-particle friction coefficient defines how difficult it is for the particles to

How to cite this article: Joseph TG, Rasimarzabadi R, Curley M. Visual Interpretation of DEM Fill Mechanisms for a Rope Shovel Dipper in Dry Broken Rock. Civil Eng Res J. 2018; 3(3): 555611. DOI: 10.19080/CERJ.2018.03.5555611

move over one another. Too low a particle friction coefficient results in particles moving easily over one another and permits the dipper structure to penetrate deeper into the dig face material. The friction coefficient in the PFC model was determined from the angle of repose calibration. However, higher friction coefficients were examined showing that an increase in friction coefficient had no significant influence on results. It is believed that the impact of the particle shape, representative of the roughness of the particles, was more significant than the value of the friction coefficient used in the model.

Contact and damping models: PFC is primarily employed for static systems. Employing these methods in dynamic models may generate unforeseen issues [13]. Different damping values were examined and those that worked best with the model were selected.

Compaction and rock particle interlock: The PFC method used to generate the dig face broken rock resulted in a low degree of particle interlock and effective material compaction; which decreased the effective frictional resistance to a dig implement. The major obstacle in this study was to create a representative broken rock dig face.

Understanding the Void Space in the Dipper

The major difference between the numerical model and the physical test observations was the degree of generation of void space at the back wall – door wall contact of the dipper. Due to the importance of understanding the generation of this void space, further simulations were performed to investigate the capability of DEM to model such a phenomenon. Shi [20] previously stated that in rope shovel dipper operation, the void space is generated at the end of the dig cycle, located at the leading edge of the dipper back wall. Shi [20] was however not aware of the filling mechanism that gave rise to the initiation of the void space.

To improve the PFC DEM model with a greater effective friction restricting the flow of particles into the dipper, previous research indicated that a mixture of fine and coarse particles reduced particle resistance to move relative to one another due to the lubrication influence of finer particles [21-23]. The revised simulation model replaced the previous uniform size distribution with a broader range of larger rock fragment material sizes.

While the revised simulations were performed with different particle sizes; other properties were kept constant. Particle sizes of 0.152m, 0.32m, and 0.8m, were trailed effectively representing small, medium, and large particle sizes, the latter medium and large sizes reflected in Figure 8. For the smallest particle size modeled at 0.152m, the same smooth flow of material as originally modeled with the broad size distribution evident in Figure 7 was discerned. In the small particle size case, little digging resistance due to a low friction coefficient was evident. Under such conditions, there exists a low likelihood of void space generation in a dipper, corresponding to a high achievable payload.

Figure 8 shows that by increasing particle size, the void space generated during the dig cycle also increases. Common with the results of the physical scale tests, the void space develops as the ingress of the dipper is blocked by incoming material. In Figure 8, rotating the dipper orientation at the end of the dig cycle caused the particles to fill the void space and generate a new void space at the front of the back wall, transitioning the void space to its final location, as was commented on by Shi [20].

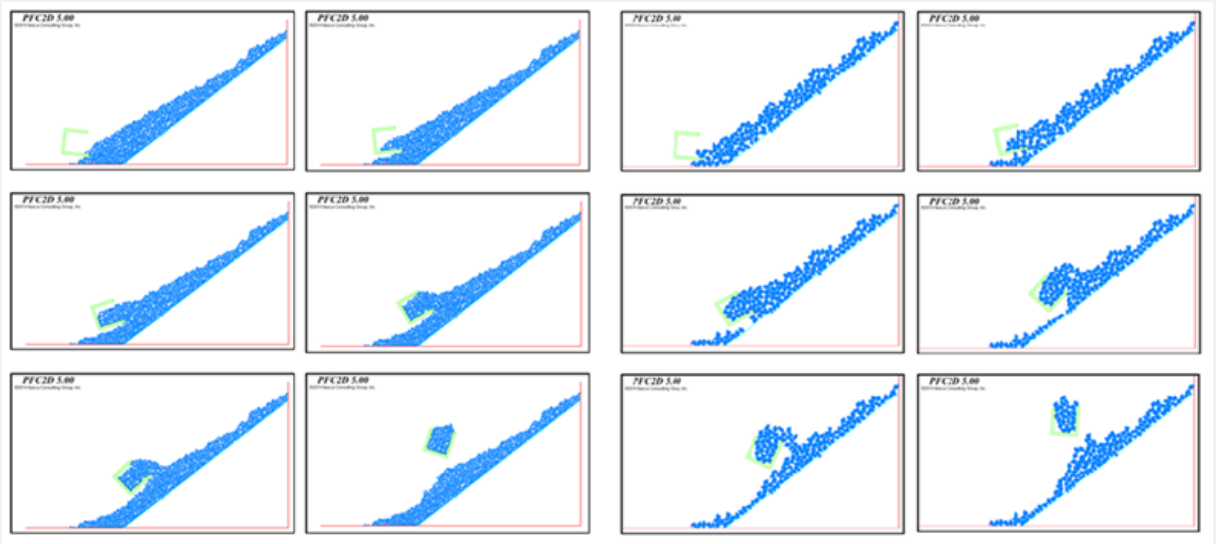

Figure 8: Simulated dig cycle with 0.32 m (left) and 0.8 m (right) particle size.

How to cite this article: Joseph TG, Rasimarzabadi R, Curley M. Visual Interpretation of DEM Fill Mechanisms for a Rope Shovel Dipper in Dry Broken Rock. Civil Eng Res J. 2018; 3(3): 555611. DOI: 10.19080/CERJ.2018.03.5555611

Figure 8 which also shows large 0.8m particle sizes, illustrates that even in rotating the dipper orientation, the material is unable to flow into the void space of the dipper due to more pronounced particle to particle interlocking, so the void space can be seen maintained in the same position to the end of the dig cycle. This is what would be logically expected for very large particle sizes.

Modifying the properties of the simulated particles in the DEM model produced results that were more representative of the physical test experience. The void space phenomenon realized in the model represented in Figure 8 is significant; as it represents the physical test evidence of Rasimarzabadi and Joseph [16], as a previously unknown dipper fill phenomenon. This knowledge now provides the impetus for dipper manufacturers to review dipper designs with the goal of negating a void space generation during the fill cycle.

To generate particles with higher frictional resistance capable of giving rise to a steeper dig face pile, particle shapes were constructed to represent moderate and high angularity materials, Figure 9. This was in turn varied via particle sizes of 0.32, 0.8, and 1.2m, then termed small, medium, and large particles, relative to the ingress across the lip system of the dipper, where the largest particle size passing was rated as being less than 1/3 of the dipper lip width, such that for a 44m3 'box' shape dipper the largest particle size is estimated at $1/33\sqrt{44}$ equivalent to 1.18m.

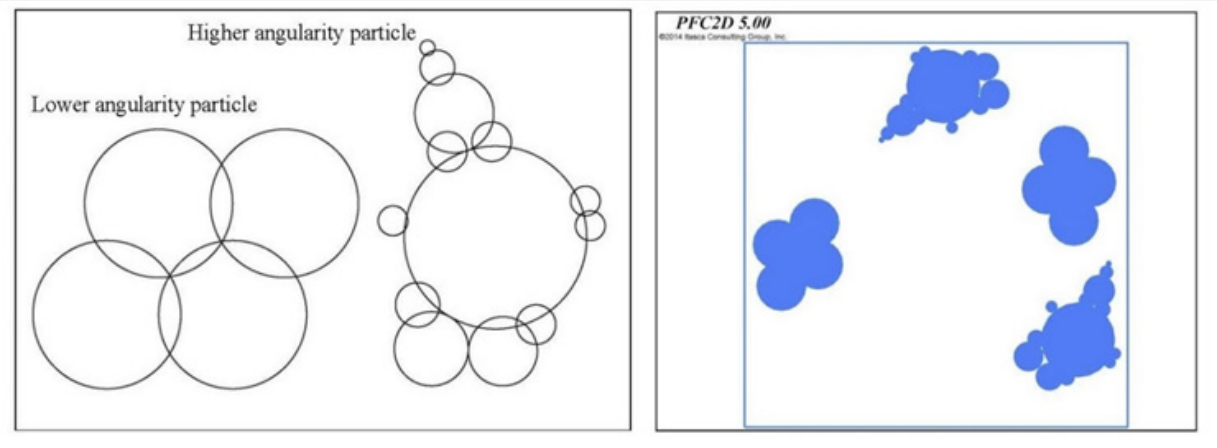

Figure 9: Refined higher angular particle clumps for PFC model.

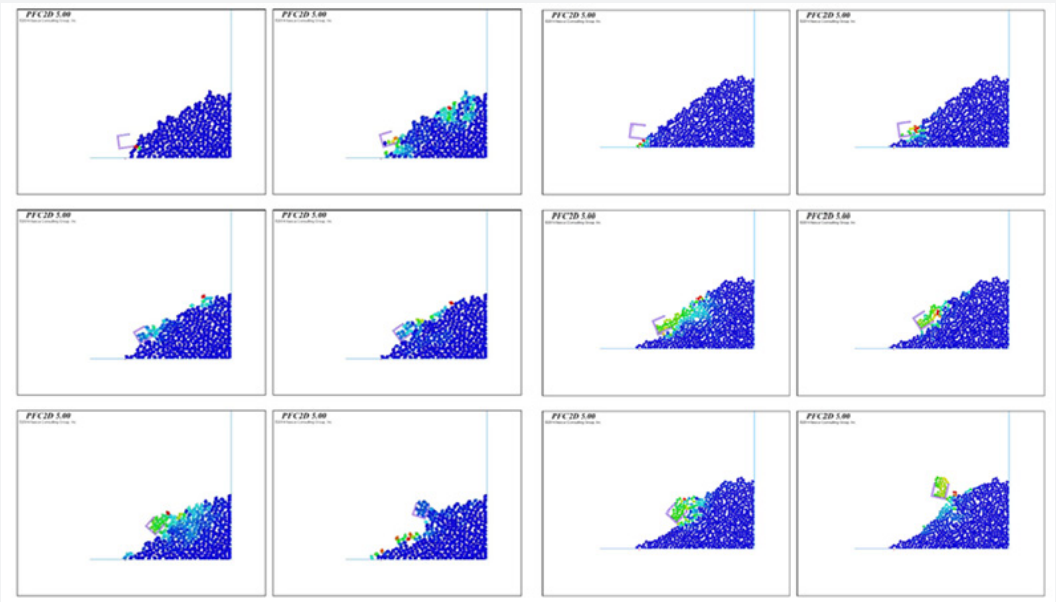

Figure 10: Dig cycles for moderate angularity large (1.2m) left and medium (0.8m) right particle size.

How to cite this article: Joseph TG, Rasimarzabadi R, Curley M. Visual Interpretation of DEM Fill Mechanisms for a Rope Shovel Dipper in Dry Broken Rock. Civil Eng Res J. 2018; 3(3): 555611. DOI: 10.19080/CERJ.2018.03.5555611

Dig piles were created using the clumps shown in Figure 9 representing moderate angularity for the three different particle sizes with the overall size distribution commensurate with the physical scale test material and field conditions. Figure 10 illustrates sample dig cycles for the large (1.2m) and medium (0.8m) particle sizes, where the blue to red colouring indicated zero (blue) to high (red) levels of induced particle motion due to the dipper - ground interaction.

As previously reported through the physical test results [16], the general particle fill flow was similar for all examined particle sizes; but the size of particles did impact dig efficiency; a function of the steepness of the dig face as the angle of repose, increasing with increasing particle size.

In Figure 10 (left) where the large particle size was roughly equal to 1/3 of the dipper lip width, at 1.2m, it is evident that during the first half of the dig cycle large particles blocked the dipper ingress restricting further particle flow into the dipper. However with changing the orientation of the dipper, gravity assisted obstructing particles moving further back into the dipper, thus permitting more material ingress. The medium 0.8m particles in Figure 10 (right) had little difficulty in flow into the dipper, reflective of an easier set of dig conditions.

As previously seen in the physical tests [16], a void space was evident in all simulations, but the void space size reduced with decreasing particle size. Commensurate with a smaller void space, as would be expected, the overall final dipper fill suggested a higher payload with smaller particle size and less likelihood of dipper ingress restriction. The results then indicated that particle size has a significant influence on loading action, highlighting the importance of blast fragmentation for excavating application.

The issue with blast fragmentation prediction is that, as illustrated in Figure 11, there is frequently an over-estimate of smaller particle size fractions compared to actual distributions inset from Figure 3. The Kuznetsov-Rosin-Rammler fragmentation model shown in Figure 11 was generated for a dolomitic limestone modulus of 15 GPa commensurate with field conditions, where a 6.25 m burden by 9 m spacing blast pattern of 235 mm diameter blast holes were loaded at 8.5 m charge length with emulsified 1.17 relative strength ANFO explosive for a 13 m bench production blast at a powder factor of 0.62 kg/m3. Although there is evidently a different size distribution particularly with reference to smaller particle sizes, the maximum size of 1.18 m for the shovel dipper was approached, and the d50 50% passing characteristic size fraction was the same at 0.3m. As such a combination of existing blast fragmentation analyses combined with the DEM model observations in this paper provides a useful tool in predicting shovel dipper interactions with fragmented rock.

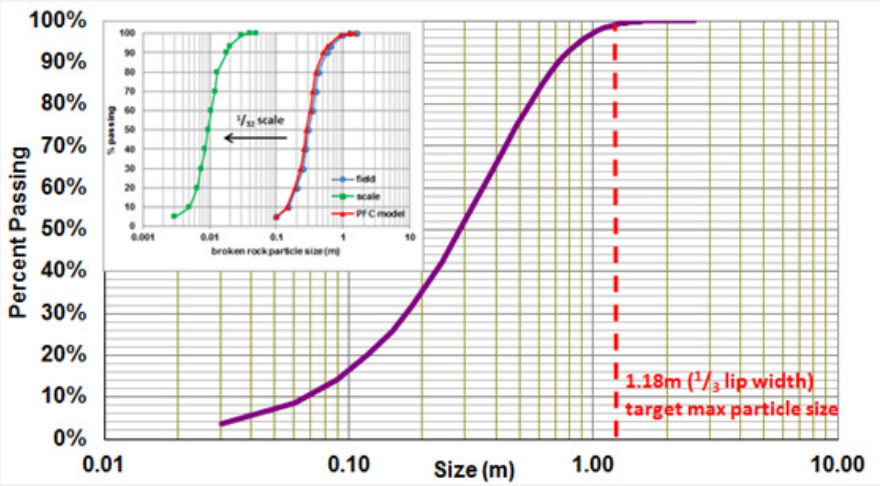

Figure 11: Sample blast fragmentation prediction compared to actual particle distribution.

To further investigate the influence of particle shape, specifically particle angularity on flow pattern, a model was generated using high angular clumps, Figure 12 then illustrates the results for the medium and large particle sizes.

Effectively the higher the angularity of the particles, the steeper the dig face pile, with the more angular particles showing a greater tendency to block the dipper ingress and promote a dipper internal void space. Figure 12 clearly shows an ingress restriction from the onset of the dig cycle. It is evident that as angularity increases, particles cannot easily pass one another and become interlocked, effectively requiring that particles overcome a higher frictional resistance due to rolling limitation.

How to cite this article: Joseph TG, Rasimarzabadi R, Curley M. Visual Interpretation of DEM Fill Mechanisms for a Rope Shovel Dipper in Dry Broken Rock. Civil Eng Res J. 2018; 3(3): 555611. DOI: 10.19080/CERJ.2018.03.5555611

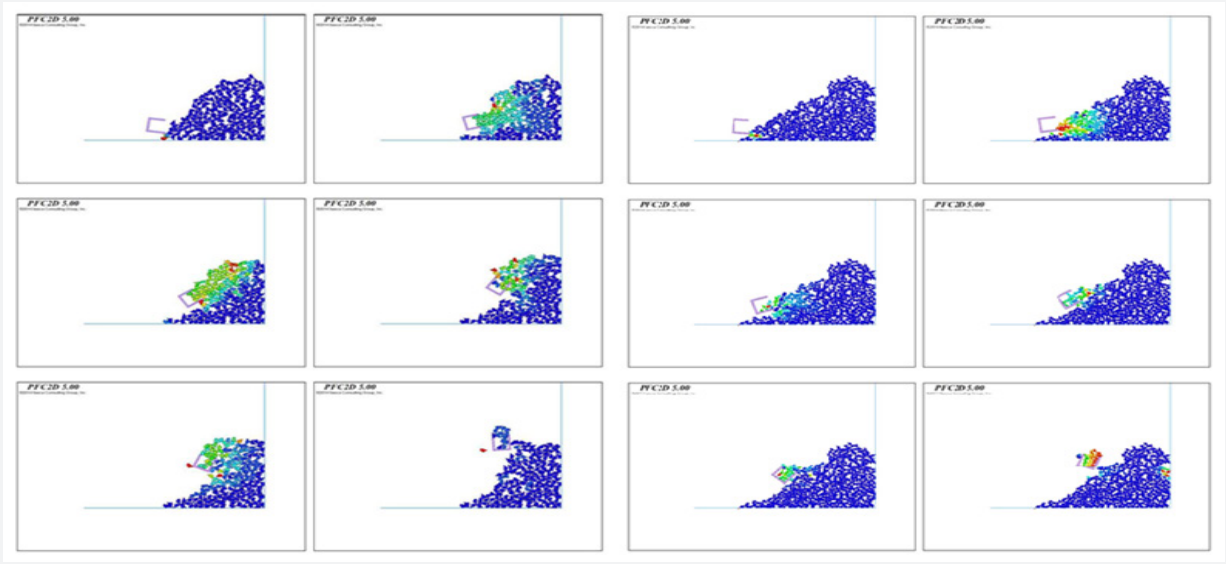

Figure 12: Dig cycle with more angular large (1.2m) left and medium (0.8m) right particle sizes.

Conclusion

A series of DEM simulations were performed to evaluate the dynamics of filling a rope shovel dipper and investigate the capability of DEM against physical test evidence commensurate with field conditions.

The modeling results showed the DEM simulation was able to mimic the broken rock particle flow noted from the physical scale tests.

The DEM simulation was shown to successfully model the flow of broken rock particles into a rope shovel dipper, predicting many of the trends seen during scale physical testing. The flow mechanism stages including particle flow layers identified in the physical tests were identifiable in the numerical simulation. The process of void space generation inside the dipper was clearly evident in the numerical simulation once the particle size, surface angularity and roughness; proportional to frictional resistance and angle of repose; were delineated through particle shape refinement in the DEM. It was specifically observed that the more fluid a digging condition observed in the simulation output, the lower opportunity to generate void space was evident, proportional to the quality of rock blast fragmentation.

References

1. Coetzee CJ, Els DNJ, Dymond GF (2010) Discrete element parameter calibration and the modelling of dragline bucket filling. Journal of Terra mechanics 47: 33-44.
2. Cleary PW (2000) DEM simulation of industrial particle flows: case studies of dragline excavators, mixing in tumblers and centrifugal mills. Powder Technology 109: 83-104.
3. Coetzee CJ, Els DNJ (2009) Calibration of discreet element parameters and the modeling of silo discharge and bucket filling, Journal of Computer and Electronics in Agriculture pp. 198-212.
4. Coetzee CJ, Els DNJ (2009) The numerical modelling of excavator bucket filling using DEM, Journal of Terra mechanics 46: 217-227.
5. Coetzee CJ, Basson AH, Vermeer PA (2006) Discrete and continuum modelling of excavator bucket filling, Journal of Terra mechanics 44: 177-186.
6. Cleary PW (1998) Discrete element modelling of industrial granular flow applications, TASK. Quarterly -Scientific Bulletin 2: 385-416.
7. Cleary P W (1998) The filling of dragline buckets, Mathematical Engineering Ind 7: 1-24.
8. Cleary PW (2004) Large scale industrial DEM modelling, Engineering Competition 21: 169-204.
9. Cleary PW (2009) Industrial particle flow modelling using discrete element method, International Journal for Computer Aided Engineering and Software 26(6): 698-743.
10. Owen DRJ, Feng YT, de Souza Neto EA, Cottrell M, Wang F, et al. (2004) The modelling of multi-fracturing solids and particulate media, International Journal for Numerical Methods in Engineering.
11. Rasimarzabadi R, Joseph TG (2016) Particle flow mechanism into rope shovel dippers, Journal of Terra mechanics 64: 10-22.
12. Tipthavonnukul S (2002) Numerical Simulation of Granular Particle Movement in Fluid Flow, PhD thesis, Department of Civil and Environmental Engineering, University of Alberta, Canada.
13. Dymond G (2007) Creation, optimization and verification of a three dimensional numerical model to simulate a dragline bucket during the digging cycle using modern DEM software, Department of Mechanical and Mechatronic Engineering, University of Stellenbosch, South Africa.
14. PFC software manual (2014) Itasca Consulting Group Inc, Canada.
15. Ghosh A, Chakraborty S (2011) Scaling laws, in Mechanics over micro and nano scales, Springer 2: 61-94.
16. Rasimarzabadi R (2016) Granular material flows into rope shovel dippers, PhD thesis, University of Alberta, Canada.
17. Majidi B (2012) Discrete element method applied to the vibration process of coke particles, MSc. thesis, Université Laval, Canada.

How to cite this article: Joseph TG, Rasimarzabadi R, Curley M. Visual Interpretation of DEM Fill Mechanisms for a Rope Shovel Dipper in Dry Broken Rock. Civil Eng Res J. 2018; 3(3): 555611. DOI: 10.19080/CERJ.2018.03.5555611

18. PFC training course (2014b) , Itasca Consulting Group Inc., Minneapolis, Minnesota, US.

19. Blouin S, Hemami A, Lipsett M (2001) Review of resistive force models for earthmoving processes, Journal of Aerospace Engineering, pp. 102-111.

20. Shi N (2007) A new approach to improving rope shovel dipper design for cutting soft rock and soils, PhD thesis, Department of Civil and Environmental Engineering, University of Alberta, Canada.

21. Singh SP, Narendrula R (2006) Factors affecting the productivity of loaders in surface mines, International Journal of Mining, Reclamation and Environment 20(1): 20-32.

22. Singh SP, Narendrula R (2006) Productivity indicators for loading equipment. CIM Journal 1: 3-7.

23. Singh SP, Glogger M, Willock D (1992) Effect of fragmentation on loader efficiency.

DOI: 10.19080/CERJ.2018.03.5555611

How to cite this article: Joseph TG, Rasimarzabadi R, Curley M. Visual Interpretation of DEM Fill Mechanisms for a Rope Shovel Dipper in Dry Broken Rock. Civil Eng Res J. 2018; 3(3): 555611. DOI: 10.19080/CERJ.2018.03.5555611